DETERMINING EFFECTS OF FERTILIZER PARTICLE SHAPE ON AERODYNAMIC PROPERTIES

J. T. Walker, T. E. Grift, J. W. Hofstee

ABSTRACT. *A method was investigated for determining the extent to which aerodynamic properties of fertilizer particles can be explained by a combination of turbulent airflow theory and a response surface involving geometric shape and mass of particles for a sample of specific fertilizer material. Fall tests were conducted, where particles were dropped and fall times were described by a mathematical model using turbulent airflow theory. Secondly, a measure of particle shape was determined to explain the difference between theoretical and measured fall times. Various dimensions of particles were measured using digital image processing. Absolute radius deviations from a preassumed best-fit circular shape were recorded and combined from two perpendicular particle images and designated "shape factor". For a sample of calcium ammonium nitrate (CAN) particles, the shape factor ranged from 11.8 to 73.0 (perfect spheres are zero). Over that range, the difference between theoretical and measured fall times was satisfactorily explained ($R^2 = 0.82$) by a function of shape factor and particle mass. A new approach to characterize a bulk of fertilizer material and its spreading properties was proposed.* **Keywords.** *Fertilizer, Granular, Spreading, Aerodynamic.*

Calibrating a granular material spreader and obtaining a pattern with an acceptable uniformity is a trial and error process affected by changes in wind speed and direction and variations in particle physical properties, such as size, size distribution, and density. Despite the effectiveness of field testing granular spreaders (Gardisser et al., 1985), it is time consuming, costly, requires specialized equipment, and must be applied to each machinaterial combination. Modeling of the granular spreading process would allow a greater understanding of the process and lead to: (a) the ability to predict the effects of variations of material properties, wind, and machine adjustments on distribution patterns; (b) the ability to develop recommendations for initial setup and calibration of specific equipment to be used with specific materials; (c) the ability to develop recommendations to granular material manufacturers for standards for particle properties of various fertilizers and pesticides; and (d) tools that could facilitate the design of equipment that would be less sensitive to critical material properties and environmental conditions. Modeling will never replace field calibration and good operating practices but should make calibration choices much less complicated.

Article was submitted for publication in March 1996; reviewed and approved for publication by the Power & Machinery Div. of ASAE in November 1996.

Work reported herein was performed as a cooperative effort at Wageningen Agricultural University.

The authors are **Joel T. Walker**, ***ASAE Member Engineer,*** Professor, **Tony E. Grift**, Graduate Assistant, Biological and Agricultural Engineering Department, University of Arkansas, Fayetteville, Ark., and **Jan Willem Hofstee**, ***ASAE Member Engineer,*** Research Engineer, Agricultural Engineering and Physics Department, Wageningen Agricultural University, Wageningen, The Netherlands. **Corresponding author:** Joel T. Walker, Biological and Agric. Engineering Dept., University of Arkansas, 203 Engineering Hall, Fayetteville, AR 72701; tel. (501) 575-2351; fax: (501) 575-2846; e-mail: <jtw@engr.uark.edu>.

Computer modeling represents the easier and more economical method of comparing materials and methods of spreading granular pesticides and fertilizers. Walker and Gardisser (1988) developed a computer model to simulate the aerial distribution of granular materials from agricultural aircraft. This model uses a fourth-order integration technique to predict the trajectories and landing points of individual particles emanating from various points on the spreader. By repeated simulations with different particle properties, a deposition pattern for a particular machine and composite granular material could be predicted. This model was used to study the basic relationships of deposition as related to particle size and wind. However, the model was verified only with general observations and not with actual machine performance. Hofstee (1993) modeled the behavior of fertilizer particles when spread with rotary and spout spreaders. He derived basic mechanical equations for particles regarded as spherical elements under the influence of centripetal, gravitational and Coriolis forces as they slide along straight vanes. To verify these predictions, he developed an ultrasonic sensor (Hofstee, 1994) capable of detecting the velocity of particles emanating from the rotor or spout. In an extension of these measurements, he predicted trajectories and ultimate deposition patterns from the machine. These modeling efforts have provided useful insights into the granular spreading process and have shown that particle shape can be an important factor in determining particle placement in the resulting deposition pattern. Therefore, good modeling of the spreading process requires a thorough knowledge of particle size and shape. Since particle mass increases as a cube of particle diameter but air drag increases only as a square of particle diameter, extra spread width is achieved for a larger particle. Just as critical to the spread pattern is the variation in particle size in the same type of material, both within a sample and from one sample to the next. Southwell and Samuel (1965) showed that in spreading fertilizer particles the variation of

material deposition between runs and across the field was partly due to the differences in fertilizer particle size distribution. Such variations in size distribution can be due to the manufacturing process or to segregation or damage during transport and handling.

Variation of individual particle shape from spherical must cause some deviation of aerodynamic performance from that of a sphere. In the past, material being spread was regarded as a composition of spherical particles without taking into account the specific properties of individual particles. The influence of measurable properties of particles on particle trajectories is virtually unknown. There is very little accurate information that correlates individual particle shape to the aerodynamic characteristics. Following the work of Mohsenin (1980), most of the work with aerodynamics has compared particles to spheres. While variations of the aerodynamic properties of fertilizer from those of spheres is recognized (Hofstee, 1992), no adequate measure of the particle shape has yet been developed. Many researchers have studied the movement of particles in an air stream to quantify the physical properties which optimize spread width. Law and Collier (1973) developed a technique for using an elutriator to measure the terminal velocity of agricultural particulates. Bilanski et al. (1962), Griffis et al. (1983), and Law and Collier (1973) showed that the larger, heavier particles would have a higher terminal velocity than smaller, lighter particles. Lee and Yates (1977) showed that particles with higher terminal velocities would travel farther than particles with a lower terminal velocity. They also showed that for a selected initial velocity, the optimum particle sizes for producing wide swaths were those having terminal velocities of 15 to 20 m/s. Yates et al. (1973) showed that terminal velocity of a material is one of the important variables affecting the maximum lateral spread. While the terminal velocity can be measured for individual particles, it is an indication of aerodynamic drag only for the single velocity. In the spreading process, particle velocity (and aerodynamic drag) can vary significantly from that of terminal velocity. Therefore, the ability to predict the aerodynamic drag based on particle shape and velocity is important to accurate modeling of particle trajectories.

The general objective of this study was to develop a model for predicting aerodynamic performance of fertilizer particles based upon physical properties of the particles. Included in this overall objective were to: (1) develop laboratory methods for describing particle size and shape; (2) explore the significance of particle shape on the aerodynamic performance of particles; (3) correlate particle shape and mathematical theory with actual fall times for particles; and (4) combine information from previous subobjectives to prescribe improvements to trajectory models.

THEORY

A theoretical model of fall times was required as a base for description of the differences in fall time caused by deviation of particle shape from spherical. The particles were assumed to behave like pseudo-spheres; therefore, deviations in fall time from that predicted for perfect spheres were assumed to be caused by shape irregularities as well as surface roughness (Grift et al., 1997). Airflow around a falling particle can be laminar (according to Stokes Law), transitional or turbulent. The drag coefficient (C_D) depends on these situations (table 1). The boundary between transitional and turbulent situations depends upon geometry of the particle. A "turbulent model" assumes that the time spent in laminar and transitional phases is negligible and therefore uses a constant drag coefficient. Earlier investigation of fall times (Hofstee, 1993; Grift et al., 1997) indicated that using a constant drag coefficient (as opposed to an iterative time-step solution in which drag coefficient varies with velocity) can introduce errors, particularly for smaller and low-density particles. However, using a constant drag coefficient allows the development of a direct solution for fall time as a function of particle radius and density and should be reasonably accurate for the major portion of mass in a fertilizer sample. The model which relates the fall distance y to a corresponding fall time t(y) is the result of solving the balance of forces around a falling sphere (Grift et al., 1997),

Table 1. Recognized conditions for different airflow regimes (adapted from Heppler, 1993)

Airflow Situation	Reynolds No.	Drag Coefficient
Laminar	$Re < 0.1$	$C_D = 24/Re$
Transitional	$0.1 < Re < 3000$	$C_D = f(Re)$
Turbulent	$3000 < Re$	C_D = constant

$$t(y) = C_1 + \frac{1}{\sqrt{gK}} \operatorname{arccosh}\left(e^{(Ky - C_2)}\right) \quad (1)$$

with

$$K = \left(\frac{1}{2}\frac{C_D A \rho_{air}}{m}\right) \quad (2)$$

Since the initial position and velocity are both zero in this study, the integration constants C_1 and C_2 are both zero; and where

m = mass (kg)
y = vertical position (m)
C_D = drag coefficient, 1
A = particle frontal area (m^2)
ρ_{air} = air density (at 20°C) (kgm^{-3})
g = local gravitational acceleration (ms^{-2})
ρ_p = particle density (kgm^{-3})
r_p = particle radius (m)

MATERIALS AND METHODS

DIGITAL IMAGING SYSTEM

In order to obtain a fast measure for non-sphericity of fertilizer particles a computerized camera arrangement was developed. It consisted of a platform (see fig. 1) for presentation of fertilizer particles, lighting, digital camera, and a PC computer with a digital imaging card. The platform was the end of a 4-mm diameter vertical plastic rod. This rod (painted flat black on the upper end) was held securely by a thumb screw in the center of a two-piece base. The center piece of the base, with the platform rod, could be rotated within the heavier, outer base piece, providing rotation of a vertical axis of a particle sitting on the flat end of the platform rod. Index marks on the two base pieces facilitated rotation of a 90° angle to provide

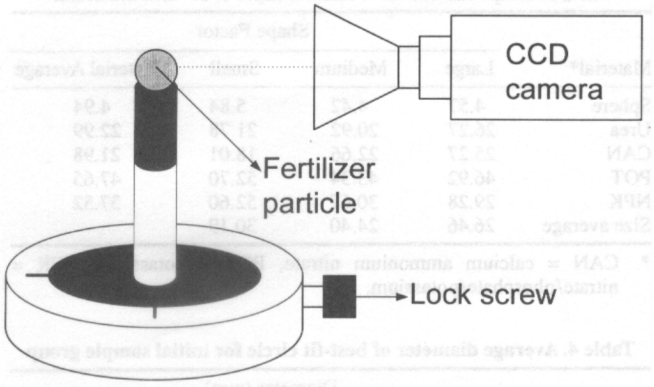

Figure 1–Platform for imaging fertilizer particles.

two perpendicular views of a particle. Lighting was provided primarily by two 6V, 2.4 W bulbs attached to plastic strips which provided support and shielded direct light from the camera lens. The bulbs were spaced to allow camera vision between and past the bulbs to the particle. Elevation of the bulbs was adjusted to provide lighting to the entire surface of a particle visible to the camera. More general lighting was from two 35W incandescent bulbs mounted vertically halfway between particle platform and lens and approximately 10 cm to each side of the vision axis. The digital camera was a monochrome COHU "Solid State Camera" Model 4722-2000/0000 with a C-mount 1:1.6/12.5-75 mm zoom lens. Camera and lens were mounted to a sturdy tripod and fixed in relation to the particle stage. The computer was a desktop PC equipped with a Vision-Plus CFG VP1300-768-E-AT (Imaging Technology Inc.) 24-bit image processing card.

Software and Method Development

Image data were captured, processed and stored under the control of a custom program written in the "C" language. The program allowed for calibration by reporting the diameter (in pixels) and image area of a sphere of known size. Calibration was adjusted with the zoom lens feature until 236 pixels/5 mm was obtained. The program also allowed for vertical placement of a horizontal cutoff line, below which visual information was not processed, effectively eliminating reflections from the platform from the image. An intensity threshold setting was made to distinguish between particle and background. The program then stored image information in memory and calculated the center of area (COA), diameters through the COA (horizontal, vertical, longest, perpendicular to longest), the longest diameter not through the COA, total area, and radii from the COA to the image edge in 360 equal-angle increments. These calculations were stored in data files for later processing.

Fall Test

Fall tests were used to determine aerodynamic properties of individual particles as described in (Grift et al., 1997). The particles were dropped by mechanical means from a platform 15.83 m high. A light sensor 5.96 cm below the drop point detected a falling particle and triggered a two-channel timer located at the bottom of the fall tube. A piezo-electric sensor fitted to a sheet metal plate sensed the impact of a particle and stopped the timer. A particle with greater aerodynamic drag showed a greater time of fall. Because of the distance between the drop point and photovoltaic sensor, a correction of 0.110 s was added to the fall times. This correction was a model prediction of the time required to fall the first 5.96 cm in still air.

Procedure

A sample of particles was selected from a sack of Calcium-Ammonium-Nitrate (CAN). Approximately 500 g of CAN were placed in a sieve stack and shaken for 10 min. Ten particles were selected randomly from each of the sieve screen sizes 4, 3.35, 2.8, 2.36, 2, and 1 mm. Only two particles were found on a 4.75 mm sieve and they were included in the sample. Thus, 62 particles were selected for analysis and image collection. After initial setup and calibration, the program was ready to collect particle image data. Particles were placed on the image analysis platform with the shortest dimension (determined visually) in the vertical axis. The platform was then rotated until the largest horizontal dimension (again, obtained visually) showed on the monitor screen. The image capture/calculation process was then initiated by the operator. An additional view of each particle was taken after rotating the platform 90°. Thus a pair of perpendicular images was processed for each particle. A sample of several images is given in figure 2.

Fall tests were conducted with the sixty-two particles. To reduce particle damage, the impact plate at the bottom of the fall test apparatus was covered with a linen cloth while testing particles from the four largest sieves. These particles were loaded into the release mechanism and dropped individually, while the fall time was recorded with a precision of 0.1 μs. The test was replicated three times for each particle or until the particle was broken by the impact. The linen cloth was then removed from the impact plate, and the three smaller groups of particles were tested in the same manner. Horizontal movement of some particles, particularly the smaller ones, resulted in the particles bouncing from the walls of the fall tube with some increase in fall time. These measurements were discarded. Some particles also broke on impact. Of the 62 original particles, data were obtained for only 54. The reproducibility of the fall test procedure was checked with nylon and PTFE spheres of 4 and 5 mm nominal diameters, dropped three times each. The standard deviation of fall time for individual spheres, indicating repeatability in the millisecond range, is given in table 2. This table also lists the equivalent drag coefficient found by back-solving the turbulent model using the average fall times.

Results and Discussion

In order to investigate the best parameter for describing particle shape, three particles each of the materials shown in table 3 were selected for image analysis. These particles were processed in the digital camera system. Initial efforts at describing particle shape from planar views involved comparison with the best-fit elliptical shapes through the ratio of the elliptical axis lengths. A spreadsheet program provided determination of the best fit ellipse through least-squared-differences between the 360 particle radii provided by the camera/program and the same radii from the elliptical equation. The average of best-fit diameters for the

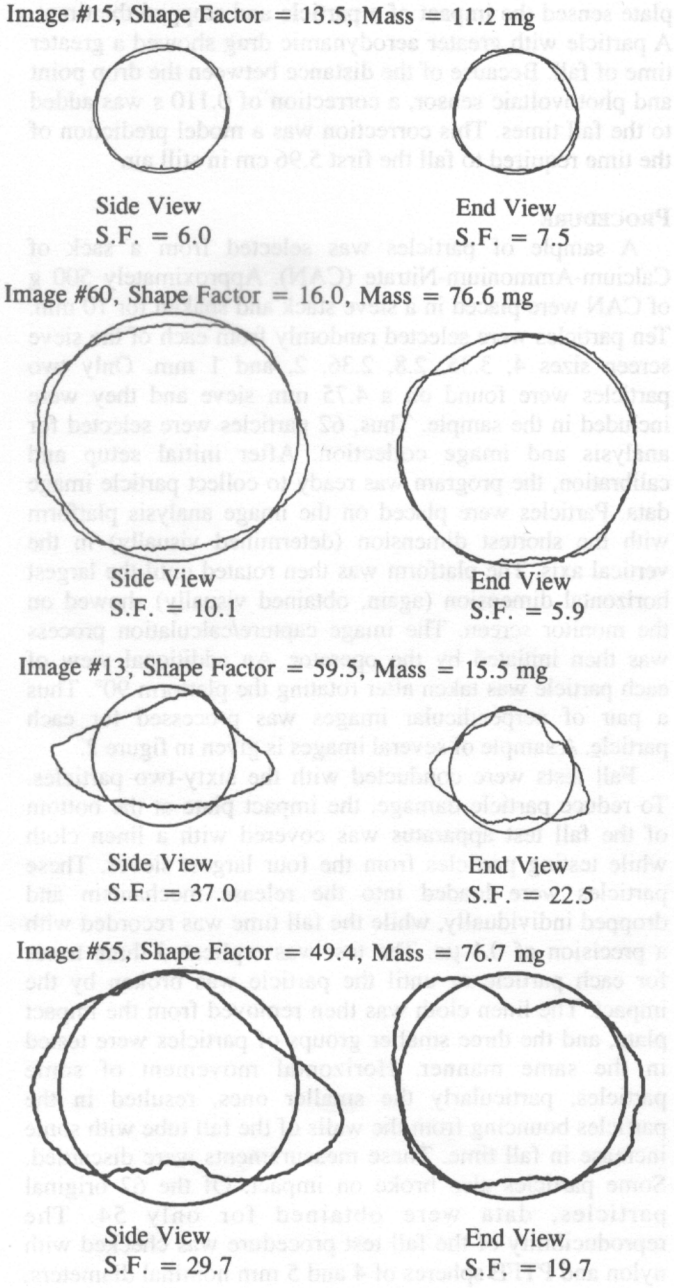

Figure 2–Sample of particle images.

initial sample of materials are given in table 4. The spreadsheet also provided the major axis ratio calculations. These early efforts provided a general measure of deviation from elliptical or spherical shape but provided little information about "roughness" or irregularity of the particles. The differences between the image and best-fit ellipse radii were next evaluated as signal data in a Fourier series expansion to produce the frequency power spectrum. For each particle image, the radius differences followed a cyclical pattern in which frequency and amplitude combined to indicate the surface "roughness" and variation from circular shape. This method proved to require too much processing time and required manual interpretation of the results. A simpler measure, roughly representing the lack-of-fit area of an image both outside and inside the best-fit circle, was calculated as the sum of the absolute values of the differences between the 360 image radii and the radii of the best fit circle. This sum was then divided by the best-fit circle diameter to obtain a dimensionless number and measures from two perpendicular views of a particle were added to obtain the value that will be called "shape factor". This addition from two views was done in order to provide more sensitivity to particles that showed roughness in both views. Shape factors for the initial sample of materials is given in table 3. Note that shape factors for spheres were not zero, due to small irregularities in the image edge due to lighting of the glossy surface and the binary nature of the radii. Visual ratings were developed for sphericity and shape of the initial sample of particles. These ratings were compared with the frequency power spectrum and shape factor data for those particles. As a result of these comparisons, "shape factor" was selected as the simpler and more effective indicator of particle shape. A MATLAB (1995) program was developed to calculate the shape factor parameter for any number of input data files.

Earlier fall tests of particles had shown a general agreement with predictions of fall times using the turbulent theory for spherical shapes (as presented in the previous section). The exception was that measured fall times were always greater than theoretical and had variations that seemed to depend upon particle shape. The processing of data then aimed at providing a measure of particle shape which could be used in correlation with the differences of fall times from the turbulent theory. Fall times were

Table 2. Average fall time and standard deviations (three replications for each sphere) of fall time for nylon and teflon (PTFE) spheres

	No. of Spheres Tested	Nominal Diameter (mm)	Average Mass (g)	Average Density (kg/m^3)	Average Fall Time (s)	Average STD of Fall Time	Equivalent C_D
Nylon	1	4	0.0465	1398	2.112163	0.000503	0.376
	3	5	0.0915	1390	2.034501	0.000730	0.354
PTFE	2	4	0.0740	2235	1.994082	0.001472	0.379
	3	5	0.1378	2200	1.949321	0.001155	0.362

Table 3. Shape factors for a small sample of several materials

	Shape Factor			
Material*	Large	Medium	Small	Material Average
Sphere	4.57	4.42	5.84	4.94
Urea	26.27	20.92	21.78	22.99
CAN	25.27	22.66	18.01	21.98
POT	46.92	43.34	52.70	47.65
NPK	29.28	30.67	52.60	37.52
Size average	26.46	24.40	30.19	

* CAN = calcium ammonium nitrate, POT = potassium, NPK = nitrate/phosphate/potassium.

Table 4. Average diameter of best-fit circle for initial sample group

	Diameter (mm)		
Material	Large	Medium	Small
Sphere	4.88	3.90	2.95
Urea	5.70	3.78	2.44
CAN	4.74	3.49	2.99
POT	4.46	3.51	2.52
NPK	4.82	3.87	2.60

graphed versus 'corresponding' diameter, as was the theoretical equation using a C_D of 0.43 (fig. 3). The 'corresponding' diameter of fertilizer particles was computed by regarding them as a sphere with a known mass and (true) density. The differences between the fall times of fertilizer particles and their theoretical counterparts were quite variable, and always greater than zero. These differences were regressed with various combinations of particle mass and shape factor in an attempt to explain the variation of fall time from theory. Finally, the RSREG and REG procedures of SAS were used to determine the best response surface involving linear, quadratic, and crossproduct combinations of mass and shape factor. The coefficients for equation 3, a direct prediction of fall times using only mass and shape factor, were also determined through regression.

Particle shape data is plotted against 'corresponding' diameter in figure 4. Nearly spherical particles had relatively low values of shape factor, while highly irregular or broken particles had relatively high values. The largest particles tended to have higher values of shape factor and were quite irregular in appearance. The points marked with square symbols instead of plus symbols were recorded as having rough fractured surfaces prior to image collection and fall tests. Other particles with non-spherical, irregular appearance also had higher values of shape factor.

The experimentally determined deviations of fall time from the turbulent theory are presented in figure 5 ("x" symbols). The deviations from theory were not constant with changing mass but tended to be greater for the smaller particles, perhaps because of the selection of theory based upon a constant drag coefficient. Particle mass and particle shape factor were used as inputs of a regression to explain the differences between actual fall time and the theoretical fall time for a sphere using a drag coefficient of 0.43. This regression took the form of a response surface (REG procedure of SAS) in which most of the difference between theory and actual measurement of fall time (residual fall time) was explained (R^2 = 0.8215). The model thus obtained was:

$$t = \beta_0 + \beta_1 S^2 + \beta_2 m_p S + \varepsilon \qquad (3)$$

where

S = shape factor, 1

m_p = mass of particle (kg)

Table 5 shows the parameters and their standard errors. The predicted residual fall time was graphed on figure 5 (+ symbols) along with the actual residuals between measurement and theory. The response surface (eq. 3) was also plotted in figure 6, in which can be seen the relative importance of mass and shape factor. Shape factor was

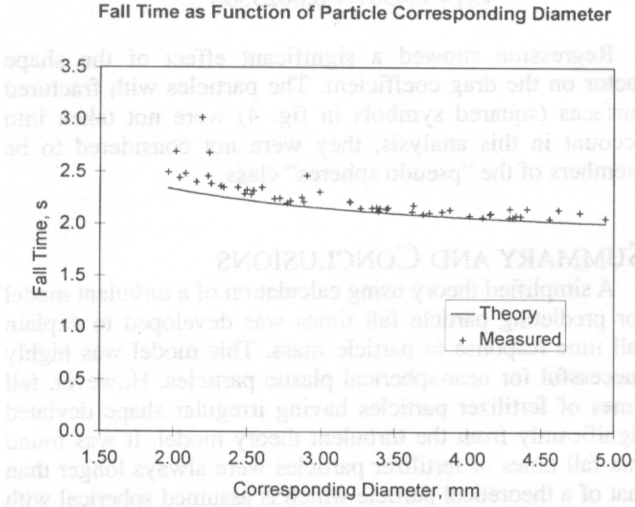

Figure 3–Theoretical (turbulent) model and measured fall times vs. 'corresponding' particle diameter for particles characterized by digital imaging technique.

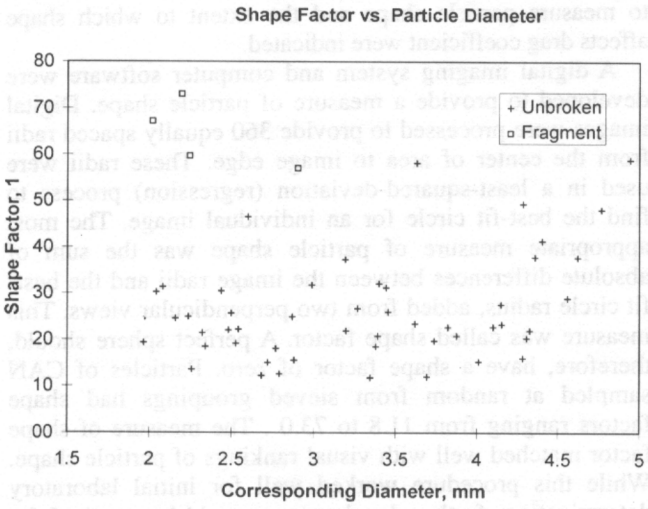

Figure 4–Particle shape factor vs. 'corresponding' particle diameter.

Table 5. Parameter estimates for model prediction of residual fall times (CAN)

Variable	Parameter	Parameter Estimate	Standard Error	Prob > |T|
Intercept	β_0	0.044476	0.00719579	0.0001
S^2	β_1	0.0000806	0.00000543	0.0001
m_pS	β_2	–0.028861	0.00464082	0.0001

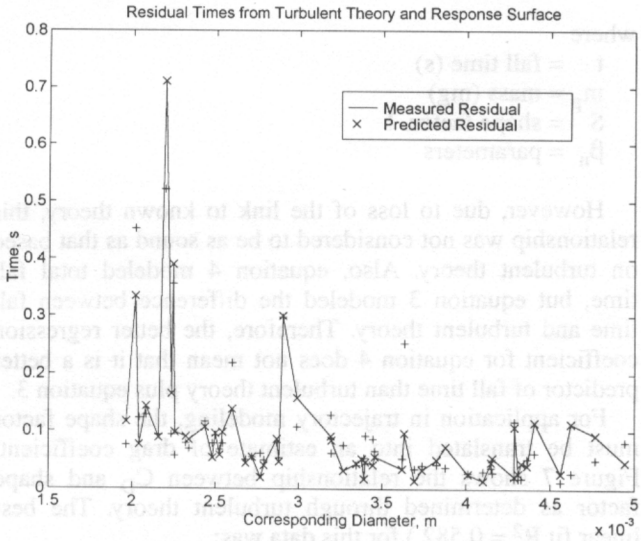

Figure 5–Deviations of fall time from turbulent model.

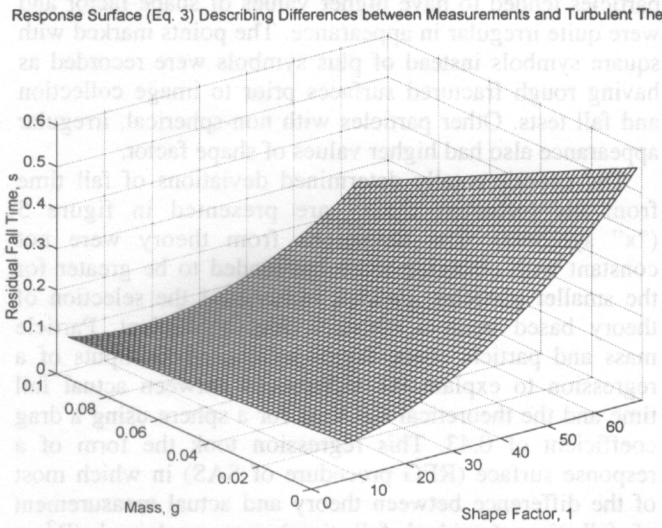

Figure 6–Response surface predicting differences (residuals) between measured and theoretical fall times.

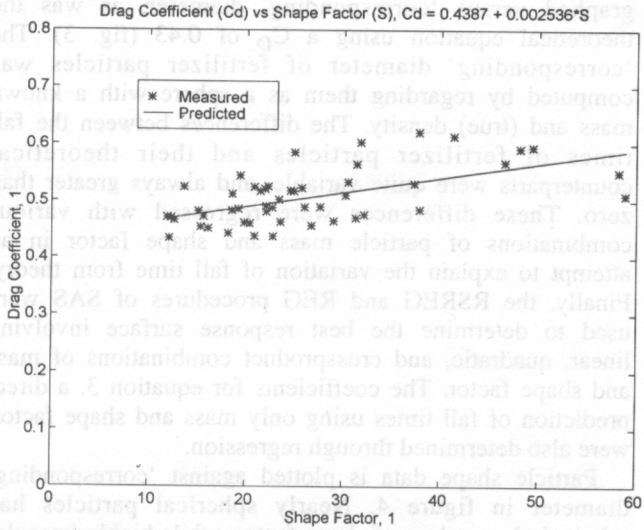

Figure 7–Drag coefficient as a function of shape factor.

quite important over the range of mass. There were no significant trends of the residuals from the response surface with respect to either the mass or shape factor. A study of the residuals from this prediction showed that the standard deviation of residuals about the response surface was 0.054 s. Analysis of standard deviation of fall times (for the particles surviving at least two falls) indicated no significant change in STD of measured fall times over the range of mass or over the range of shape factor. The STD of measured fall times from individual particles was averaged for all particles and found to be 0.019 s, which is an indication of the purely random component of the fall time data (about 35% of 0.054 s, the STD of residuals about the response surface). Thus, the modified theory accounted for a major portion of the non-random variation in fall time.

Efforts to directly explain the fall times (without a turbulent theory base) in a non-linear regression involving mass and particle shape were also successful. The best form of the direct fall time prediction equation ($R^2 = 0.91$) was:

$$t = \beta_0 + \beta_1 m_p^{B_2} + \beta_3 S^2 + \beta_4 m_p S + \varepsilon \qquad (4)$$

where

t = fall time (s)
m_p = mass (mg)
S = shape factor, 1
β_n = parameters

However, due to loss of the link to known theory, this relationship was not considered to be as sound as that based on turbulent theory. Also, equation 4 modeled total fall time, but equation 3 modeled the difference between fall time and turbulent theory. Therefore, the better regression coefficient for equation 4 does not mean that it is a better predictor of fall time than turbulent theory plus equation 3.

For application in trajectory modeling, the shape factor must be translated into an estimate of drag coefficient. Figure 7 shows the relationship between C_D and shape factor as determined through turbulent theory. The best linear fit $R^2 = 0.582$) for this data was:

$$C_D = 0.4387 + 0.002536S$$

Regression showed a significant effect of the shape factor on the drag coefficient. The particles with fractured surfaces (squared symbols in fig. 4) were not taken into account in this analysis, they were not considered to be members of the "pseudo spheres" class.

Summary and Conclusions

A simplified theory using calculation of a turbulent model for predicting particle fall times was developed to explain fall time response to particle mass. This model was highly successful for near-spherical plastic particles. However, fall times of fertilizer particles having irregular shape deviated significantly from the turbulent theory model. It was found that fall times of fertilizer particles were always longer than that of a theoretical particle which is assumed spherical with equal mass and density and $C_D = 0.43$. It was concluded that a combination of particle shape and surface roughness contributed significantly to the aerodynamic properties. Since drag coefficient is critical to developing accurate trajectory models of individual particles, studies of methods to measure particle shape and the extent to which shape affects drag coefficient were indicated.

A digital imaging system and computer software were developed to provide a measure of particle shape. Digital images were processed to provide 360 equally spaced radii from the center of area to image edge. These radii were used in a least-squared-deviation (regression) process to find the best-fit circle for an individual image. The most appropriate measure of particle shape was the sum of absolute differences between the image radii and the best-fit circle radius, added from two perpendicular views. This measure was called shape factor. A perfect sphere should, therefore, have a shape factor of zero. Particles of CAN sampled at random from sieved groupings had shape factors ranging from 11.8 to 73.0 . The measure of shape factor matched well with visual rankings of particle shape. While this procedure worked well for initial laboratory determination, further development would be required for analysis of more numerous or larger samples. The

limitations were manual placement of particles on the platform, sensitivity to lighting position, and a multi-step data processing procedure.

Fall time of fertilizer particles was more accurately explained by a combination of turbulent airflow theory and an equation involving particle shape factor and mass. The equation involving particle shape and mass explained the residual fall time after turbulent theory with $R^2 = 0.82$. Repeated fall time measurements on individual particles indicated that much of the fall time variation that remained unexplained by particle mass and shape information was random in nature. Further work to characterize particle shape and the effects on aerodynamic properties of individual particles is recommended for other common fertilizer materials.

These methods for measuring shape factor and models for determining drag coefficient or fall times will be used in refinement of particle trajectory models. Inclusion of correction for particle shape in these models will give more accurate prediction of spreader-to-target trajectories than were previously attainable, allowing adjustments to equipment design parameters. Such models will also indicate the importance of the fertilizer material in the distribution process and could indicate a need for greater control on particle size or shape variation in the bulk material. Models of particle trajectories must be validated to be useful and a device to launch particles at known velocity and direction was developed for that purpose (Grift and Hofstee, 1997).

Acknowledgments. The authors wish to thank Mr. Pieter Everts for his assistance in data collection, Mr. Siem Bak for his role in developing imaging software, and Dr. Gerrit Gort for his valuable assistance with statistical analysis. Thanks from Dr. Walker to all those at Wageningen Agricultural University who made possible an enjoyable and productive sabbatical visit.

References

Bilanski, W. K., S. H. Collins and P. Chu. 1962. Aerodynamic properties of seed grains. *Agricultural Engineering* 43(3):216-219.

Gardisser, D. R., J. T. Walker and M. L. Purdy. 1985. Evaluation and calibration of agricultural aircraft spreading dry materials. ASAE Paper No. AA85-005. St. Joseph, Mich.: ASAE.

Griffis, C. L., D. W. Ritter and E. J. Mathews. 1983. Simulation of rotary spreader distribution patterns. *Transactions of the ASAE* 26(1):33-37.

Grift, T. E., J. T. Walker and J. W. Hofstee. 1997. Aerodynamic properties of individual fertilizer particles. *Transactions of the ASAE* 40(1):13-20.

Grift, T. E. and J. W. Hofstee. 1997. Development of a fertilizer particle accelerator. *J.Agric. Eng. Res.* (In review).

Heppler, K. 1993. Parameterstudien zur Granulatausbringung mit Schleuderscheiben (Study of parameters affecting granular fertilizer spreading with vane-type spreaders), diss. Karlsruhe, Germany: Universität Karlsruhe.

Hofstee, J. W. 1992. Handling and spreading of fertilizers: Part 2, Physical properties of fertilizer, measuring methods and data. *J. Agric. Eng. Res.* 53(2):141-162.

————. 1993. Physical properties of fertilizer in relation to handling and spreading, diss. Wageningen, The Netherlands: Wageningen Agricultural University.

————. 1994. Handling and spreading of fertilizers: Part 3, Measurement of particle velocities and directions with ultrasonic transducers,theory, measurement system, and experimental arrangements. *J. Agric. Eng. Res.* 58(1):1-16.

Law, S. E. and J. A. Collier. 1973. Aerodynamic resistance coefficients of agricultural particulates determined by elutriation. *Transactions of the ASAE* 16(5):918-921.

Lee, K. C. and W. E. Yates. 1977. A rotary cylinder spreader for aircraft granular applications. *Transactions of the ASAE* 20(5):801-805.

MATLAB Version 4.2. 1995. Natick, Mass.: The Math Works Inc.

Mohsenin, N. N. 1980. *Physical Properties of Plant and Animal Materials*. New York, N.Y.: Gordon & Breach, Science Publishers, Inc.

Southwell, P. H. and J. Samuel. 1965. The accuracy of fertilizer metering by full-width machines. In *Proc. of the 41st Annual Meeting of the Council on Fertilizer Application*. VI:1-12.

Walker, J. T. and D. R. Gardisser. 1988. Modeling fertilizer particle trajectories. ASAE Paper No. AA88-003. St. Joseph, Mich.: ASAE.

Yates, W. E., J. Stephenson, K. Lee and N. B. Akesson. 1973. Dispersal of granular materials from agricultural aircraft. *Transactions of the ASAE* 16(2):609-614.